Extension of quasi-load insensitive generalized Class-E Doherty operation with complex load trajectories

Mehdi Otmani, Ayssar Serhan, Jean-Daniel Arnould, Estelle Lauga-Larroze, Pascal Reynier, Alexandre Giry

chips

MDPI

Article

Extension of Quasi-Load Insensitive Generalized Class-E Doherty Operation with Complex Load Trajectories

Mehdi Otmani [1], Ayssar Serhan [1], Jean-Daniel Arnould[2], Estelle Lauga-Larroze[2], Pascal Reynier[1] and Alexandre Giry[1]

[1] Univ. Grenoble Alpes, CEA, LETI, 38054 Grenoble, France; {mehdi.otmani; ayssar.serhan; alexandre.giry; pascal.reynier}@cea.fr
[2] Univ. Grenoble Alpes, CNRS, Grenoble INP, TIMA 38000 Grenoble, France; {jean-daniel.arnould; estelle.lauga-larroze}@univ-grenoble-alpes.fr

Abstract: This paper extends the quasi-load insensitive (QLI) Class-E Doherty power amplifier (PA) design methodology to address Doherty PA combiners with complex load impedance trajectories. Additionally, the QLI operation is analyzed for generalized class-E output matching network taking into account an input series inductance. The analysis of the Class-E PA power and efficiency load-pull contours shows that changing the class-E output matching network resonance factor and the input series inductance allows rotating the loadpull contours to achieve QLI operation with various Doherty combiners. Moreover, a modified class-E output network is proposed to overcome the frequency limitation that might be caused by the class-E network resonance factor choice. The impact of the resonance factor and the series inductance on the auxiliary off-state impedance is studied. To validate the proposed methodology, a 40 W Doherty PA is designed and simulated using commercial GaN HEMT transistors achieving more than 70% Efficiency over 6-dB output power back-off at 3.8 GHz.

Keywords: Generalized Class-E; Quasi-load Insensitive; Power Amplifier; Load Modulation; Doherty; Bond Wire; off-state impedance, Class-E.

1. Introduction

Modern wireless communication systems use complex modulated signals with high instantaneous bandwidth to improve spectral efficiency and data rate. These signals exhibit high peak-to-average power ratio (PAPR) which require high back-off from the saturation power to meet the system linearity requirement, consequently degrading the average efficiency of conventional PAs. In addition, 5G transceivers need to address an increased number of frequency bands strengthening the efficiency-bandwidth trade-off challenge in 5G PAs [1].

To increase the PA efficiency under high output power back-off (OBO), supply modulation (Envelop Tracking) and load modulation (Doherty, Outphasing...) PA architectures have been developed [1] [2] [3]. For cellular wireless infrastructure applications, the wide adoption of conventional Doherty PA (DPA) gave birth to several variants and design approaches enabling increased OBO range [4], extended operating bandwidth [5] [6] [7] and compact size [8]. The QLI class-E DPA proposed in [6] shows promising efficiency and bandwidth performance. However, the analysis proposed in [6] only considers DPA combiners with pure real load impedances trajectories and does not address the case of DPA combiners with complex impedance trajectories as the one proposed in [8].

In this paper, the QLI class-E methodology is revisited and extended to enable QLI operation for Doherty combiners with complex load impedance trajectories. Moreover, the proposed analysis shows that QLI behavior can be achieved for generalized class-E

Citation: To be added by editorial staff during production.

Academic Editor: Firstname Lastname

Received: date
Revised: date
Accepted: date
Published: date

network taking into account an input series inductor. Furthermore, the maximum operating frequency is discussed and a modified class-E network configuration is proposed to overcome the maximum operating frequency limitation that might be caused by the class-E network resonance factor choice and the input series inductor. Finally, the impact of the resonance factor and the input series inductor on the auxiliary off-state impedance is investigated. The proposed analysis is demonstrated in simulation on a 40 W Doherty PA using commercial GaN HEMT devices at 3.8 GHz.

2. Generalized Class-E Output Network

The class-E output network with finite DC-feed inductor, **Figure 1**, is commonly used due to its simplicity and straightforward parameters calculation. The inductor $\boldsymbol{L_1}$ provides the DC current to the device during the on-state and contributes along with the capacitance $\boldsymbol{C_1}$ to ensure the AC current flow to the output during the off-state. The series reactance $\boldsymbol{jX}$ is used to adjust the phase of the output current as to avoid current and voltage waveforms overlap at the device drain plane. Finally, the $\boldsymbol{L_0 - C_0}$ filter is used to filter out the harmonics and achieve a sinusoidal output. The generalized Class-E network considers a series inductance $\boldsymbol{L_b}$ between $\boldsymbol{L_1}$ and $\boldsymbol{C_1}$. $\boldsymbol{L_b}$ can be used to take into account a bond wire inductance as it become significantly high at microwave frequency.

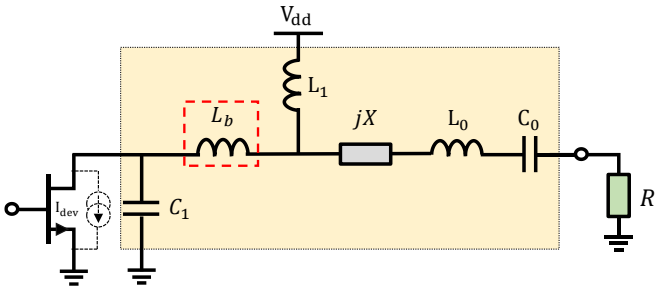

Figure 1. Generalized class-E output network.

The analytical solution of the generalized class-E network are given in [9]. The network parameters $\{\boldsymbol{R}, \boldsymbol{L_b}, \boldsymbol{X}, \boldsymbol{L_1}, \boldsymbol{C_1}\}$ depend on the supply voltage ($\boldsymbol{V_{dd}}$), the target output power ($\boldsymbol{P_{out}}$), the resonance factor $\boldsymbol{q = f_1/f_0}$ with $\boldsymbol{f_0}$ the design frequency, $\boldsymbol{f_1}$ the resonance frequency of $\boldsymbol{L_1 - C_1}$ network and $\boldsymbol{\alpha = L_b/L_1}$. Note that the equations [9, eq. (16)] and [9, eq. (17)] have typo errors. The corrected equations are given in (1) and (2):

$$C_2 = \left[\frac{\pi}{Q}\cos\left(\frac{\pi}{Q}\right) - \sin\left(\frac{\pi}{Q}\right)\right] - \frac{Qp}{Q^2-1}\left[\frac{\cos(\phi)}{Q}\sin\left(\frac{\pi}{Q}\right) + \frac{Q^2-2}{Q^2}\sin(\phi)\cos\left(\frac{\pi}{Q}\right)\right] \quad (1)$$

and

$$\tan\phi = \frac{\pi + \pi\cos\left(\frac{\pi}{Q}\right) + 2Q\sin\left(\frac{\pi}{Q}\right)}{2(Q^2-1)\left[1-\cos\left(\frac{\pi}{Q}\right)\right] + Q\pi\sin\left(\frac{\pi}{Q}\right)} \quad (2)$$

The network parameters are expressed as follows [9] :

$$R(\alpha,q) = \frac{K_P(\alpha,q)\,V_{dd}^2}{P_{out}} \qquad C_1(\alpha,q) = \frac{K_c(\alpha,q)}{\omega_0\,R(\alpha,q)}$$

$$X(\alpha,q) = \frac{K_x(\alpha,q)\,R(\alpha,q)}{\omega_0} \qquad L_1(\alpha,q) = \frac{K_L(\alpha,q)\,R(\alpha,q)}{\omega_0} \quad (3)$$

$$L_0(\alpha,q) = \frac{Q_L R(\alpha,q)}{\omega_0} \qquad C_0(\alpha,q) = \frac{1}{L_0(\alpha,q)\,\omega_0^2}$$

The analytical expression of $\boldsymbol{K_L, K_C, K_x, K_P}$ are expressed in [9] as a function of $\boldsymbol{\alpha}$ and $\boldsymbol{q}$ considering an ideal squared input signal drive with 50% duty-cycle. $\boldsymbol{Q_L}$ is the loaded quality factor of the $\boldsymbol{L_0 - C_0}$ filter. Note that, in this article Q_L is considered infinite to filter the harmonics to obtain ideal class-E waveform.

The coefficient $\boldsymbol{K_L, K_C, K_x}$ and $\boldsymbol{K_P}$ are plotted in **Figure 2** versus $\boldsymbol{q}$ and for different value of $\boldsymbol{\alpha}$. It is important to highlight that $\boldsymbol{\alpha \geq 0}$ and $\boldsymbol{0 < q \leq 2}$. As it can be noticed in **Figure 2**, the value of $\boldsymbol{K_L}$ and $\boldsymbol{K_X}$ increases drastically for low $\boldsymbol{q}$ and high $\boldsymbol{\alpha}$ making the value of $\boldsymbol{L_1}$ and $\boldsymbol{jX}$ unsuitable for practical design.

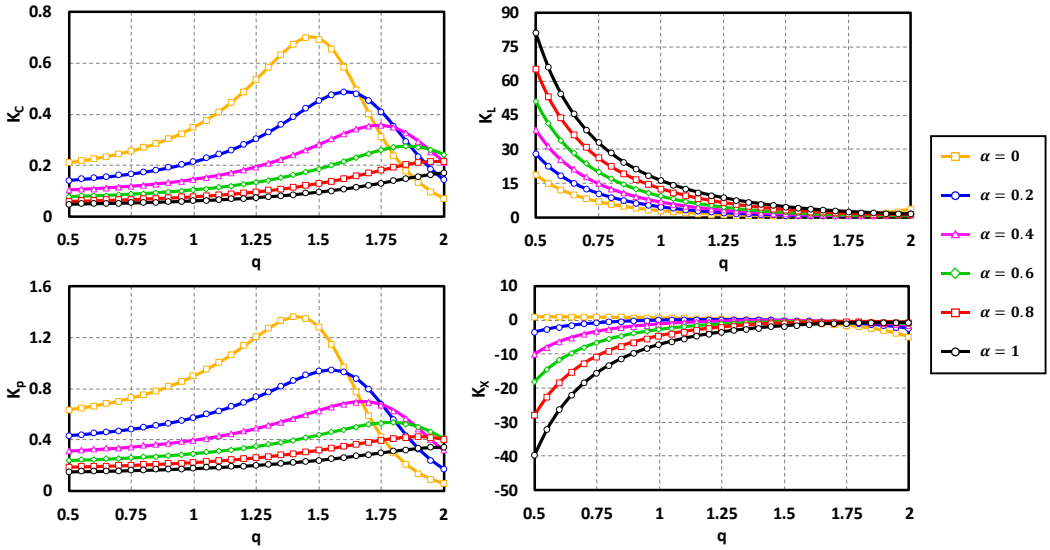

Figure 2. K_L, K_C, K_x *and* K_P for $q = [0.5: 2]$ and $\alpha = [0: 1]$.

In [6] [7], the QLI class-E operation is only expressed for the specific case of $\boldsymbol{\alpha = 0}$ (i.e. $\boldsymbol{L_b = 0}$) and the coefficients $\boldsymbol{K_L, K_C, K_x, K_P}$ were expressed versus $\boldsymbol{q}$ using polynomial fitting functions of the numerical solution [10]. Note that, this article is the extension of [11] where the results were extracted using the fitted coefficients $\boldsymbol{K_L, K_C, K_x, K_P}$. In the following, the same analysis as [11] is proposed and extended using the analytical solution.

3. Quasi-Load Insensitive Class-E Doherty Operation

3.1 Original QLI Class-E ($\boldsymbol{q = 1.33}$ and $\boldsymbol{\alpha = 0}$) DPA Design Methodology

The original QLI class-E Doherty design methodology, presented in [6] [7], consists of using two identical class-E PAs for the Main and Auxiliary devices with a specific finite DC-feed inductance network solution ($\boldsymbol{q = 1.33}$) considering no series inductance ($\boldsymbol{L_b = 0}$) and combines them using a Conventional or Wideband Doherty combiner, **Figure 3** (a). The use of QLI denomination is related to the impedance trajectories of the DPA moving along the power contours (i.e., the real-impedance axis) while laying inside high-efficiency regions. To illustrate this, the normalized $\boldsymbol{P_{out}}$ and the efficiency loadpull contours of a class-E PA with finite DC-feed inductance network using $\boldsymbol{q = 1.33}$ are plotted on **Figure 3** (b). Note that loadpull is applied at the output of the class-E network and not at the drain plane of the transistor. Moreover, the load trajectories of a conventional and wideband Doherty combiner are plotted considering a target output back-off of 6dB ($\boldsymbol{\zeta = 4}$). Note that, herein and for all subsequent graphs, the smith chart is normalized to $\mathbf{R(\alpha, q)}$. The load reflection coefficient $\boldsymbol{\Gamma_L}$ is given by (4) ,where $|\boldsymbol{\Gamma_L}|$ and $\boldsymbol{\theta_L}$ are the magnitude and phase of $\boldsymbol{\Gamma_L}$.

$$\Gamma_L = \frac{Z_L - R(\alpha, q)}{Z_L + R(\alpha, q)} = |\Gamma_L| e^{j\theta_L} \quad (4)$$

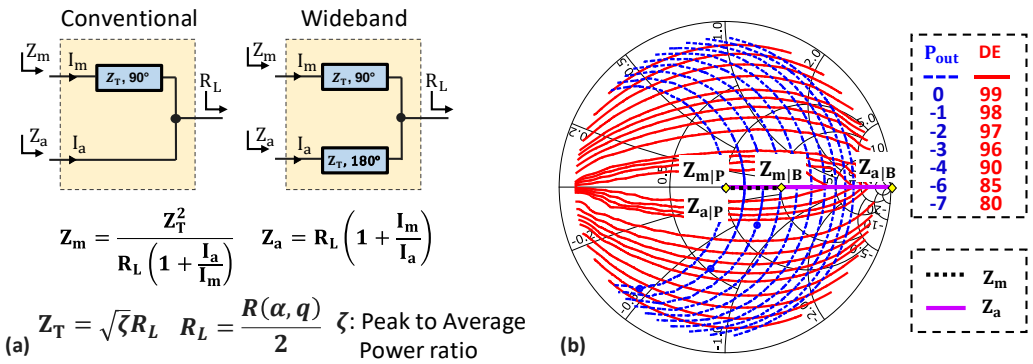

Figure 3. (a) Conventional and Wideband Doherty combiners (b) load trajectories of the Conventional 6-dB Doherty combiner and loadpull contours for q = 1.33.

As shown on **Figure 3** (b), the load impedance seen by the Main PA at back-off power ($\boldsymbol{Z_{m|B} = 2 \times R, \Gamma_{m|B} = 0.33}$) and at peak power ($\boldsymbol{Z_{m|P} = R}$, $\boldsymbol{\Gamma_{m|P} = 0}$) belongs to power contours with a 3dB ratio (as expected for **ζ = 4**) and are within the Drain Efficiency (DE) contours DE>95%. Similarly, the load impedance seen by the Auxiliary PA at peak output power reaches the maximum efficiency region, i.e., $\boldsymbol{Z_{a|P} = Z_{m|P} = R}$, $\boldsymbol{\Gamma_{m|P} = \Gamma_{a|P} = 0}$. The QLI class-E ($\boldsymbol{q = 1.33}$) DPA proposed in [6]**, Figure *4* (a),** is validated using large signal simulation considering idealized large signal transistors model considering a device output capacitance presented in **Figure *4* (a)**. Note that the output capacitance of the device, $\boldsymbol{C_{dev}}$, has to be smaller than the parallel capacitance, $\boldsymbol{C_1}$, of the network otherwise the class-E operates in suboptimum and the performances are degraded. The simulation results plotted in **Figure 4 (b)** shows that high efficiency Doherty operation is achieved for 6dB OBO.

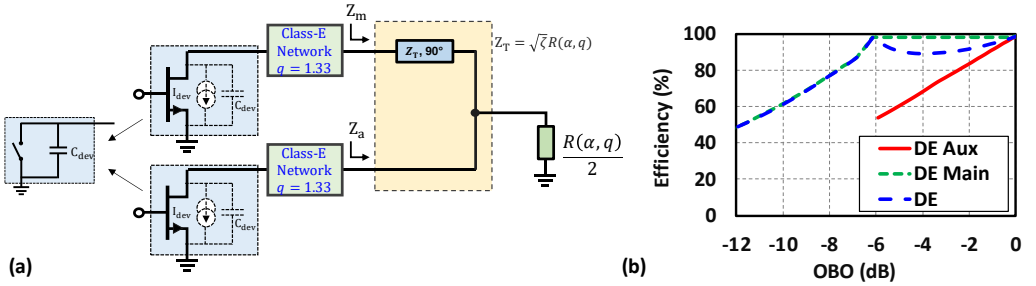

Figure 4. (a) Original QLI DPA proposed in *[6]***.** *(b)* Efficiency versus OBO for QLI Doherty PA (q=1.33).

Therefore, the Original QLI class-E approach appears to be an effective solution to enhance the efficiency of Doherty PA. In the following subsection, we extend the Original QLI class-E operation for complex to real impedance trajectory to address other types of Doherty combiners.

3.2 Extension of QLI Class-E DPA Methodology

The QLI class-E Doherty PA design methodology presented in the previous section applies only for Doherty combiners having pure-real load impedances trajectories. These combiners usually involve one or more quarter-wave transmission line [2] [5]**,** which makes them unsuitable for compact integrated power amplifiers. In order to achieve compact design, a compact L-C Doherty combiner has been proposed in [8] [12], **Figure 5** (a). This LC combiner is particularly interesting when using class-E Main and Auxiliary PAs since the combiner components can be merged with the class-E output network elements

[8]. However, the impedances $\boldsymbol{Z_m}$ and $\boldsymbol{Z_a}$ seen by the Main and Auxiliary PAs are no more pure-real and follow complex impedance trajectories, **Figure 5** (b). Hence, the Original QLI methodology with $\boldsymbol{q = 1.33}$ cannot be applied efficiently.

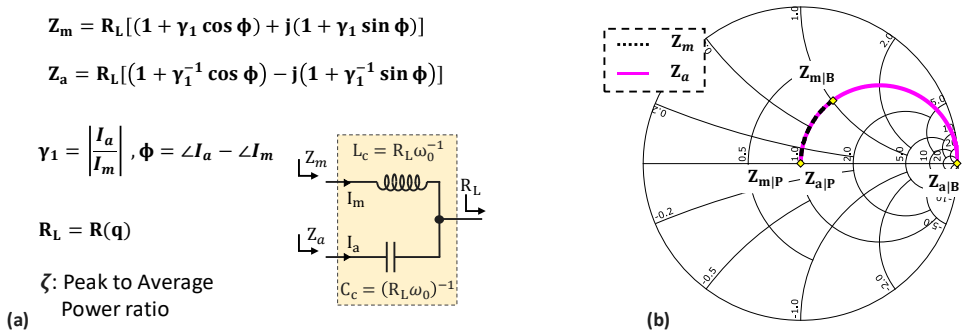

Figure 5. (a) L-C Doherty combiner. (b) Load trajectories of 6-dB LC Doherty combiner.

To extend the QLI Class-E design methodology for Doherty combiners with complex impedance trajectories, we propose to investigate the output power and efficiency load-pull contours of class-E PA for different $\boldsymbol{q}$ values. Note that $\boldsymbol{P_{out}}$ is normalized to the output power when presenting $\boldsymbol{R(\alpha, q)}$. For sake of simplicity, we first deal with the case of $\boldsymbol{\alpha = 0}$. then, the impact of $\boldsymbol{\alpha}$ will be discussed. As shown in **Figure 6**, increasing the resonance factor $\boldsymbol{q}$ rotates the loadpull contours in the clockwise direction and vice versa. Note that the alignment between the efficiency and $\boldsymbol{P_{out}}$ contours remain the same regardless of $\boldsymbol{q}$. Hence, the QLI class-E operation can be achieved for complex impedance trajectories. For instance, selecting $\boldsymbol{q = 0.9}$ allows to align the QLI high-efficiency region with the impedance trajectories of the L-C Doherty combiner presented on **Figure 5** (b). Moreover, it is now possible to select any $\boldsymbol{q}$ value and use the generalized combiner synthesis technique proposed in [3] to synthesize the required combiner.

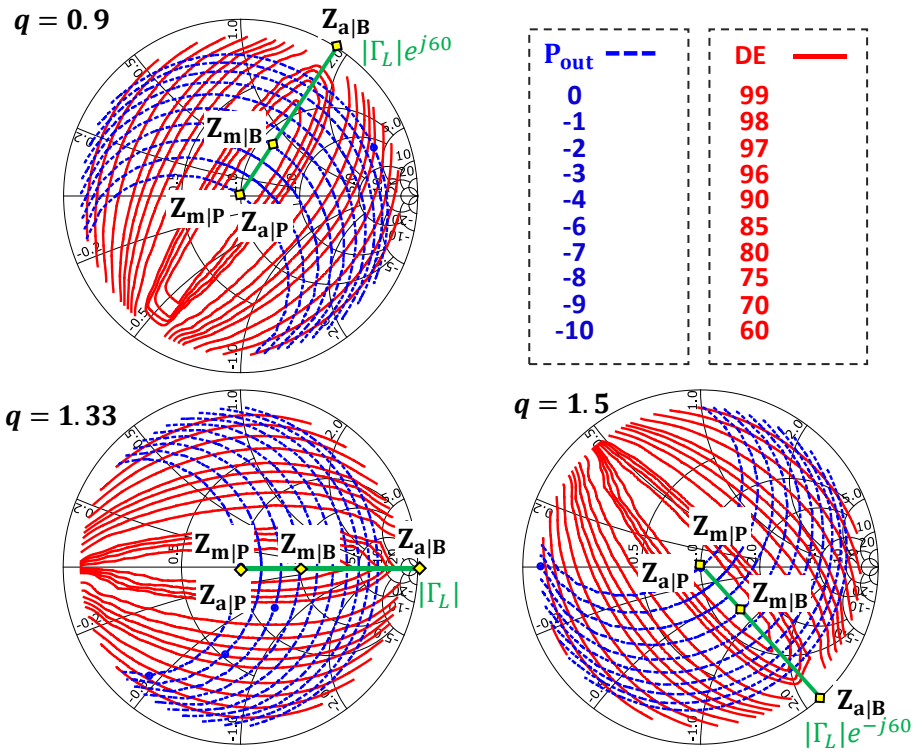

Figure 6. Efficiency and normalized output power contours for various resonance factor q, normalize to $R(\alpha, q)$.

The loadpull contours in **Figure 6** can be represented differently by plotting the efficiency and output power versus $\boldsymbol{q}$ sampled at different $|\boldsymbol{\Gamma_L}|$ and for a given $\boldsymbol{\theta_L}$, as shown on **Figure 7**. The sampled Γ_L are illustrated in **Figure *6***.

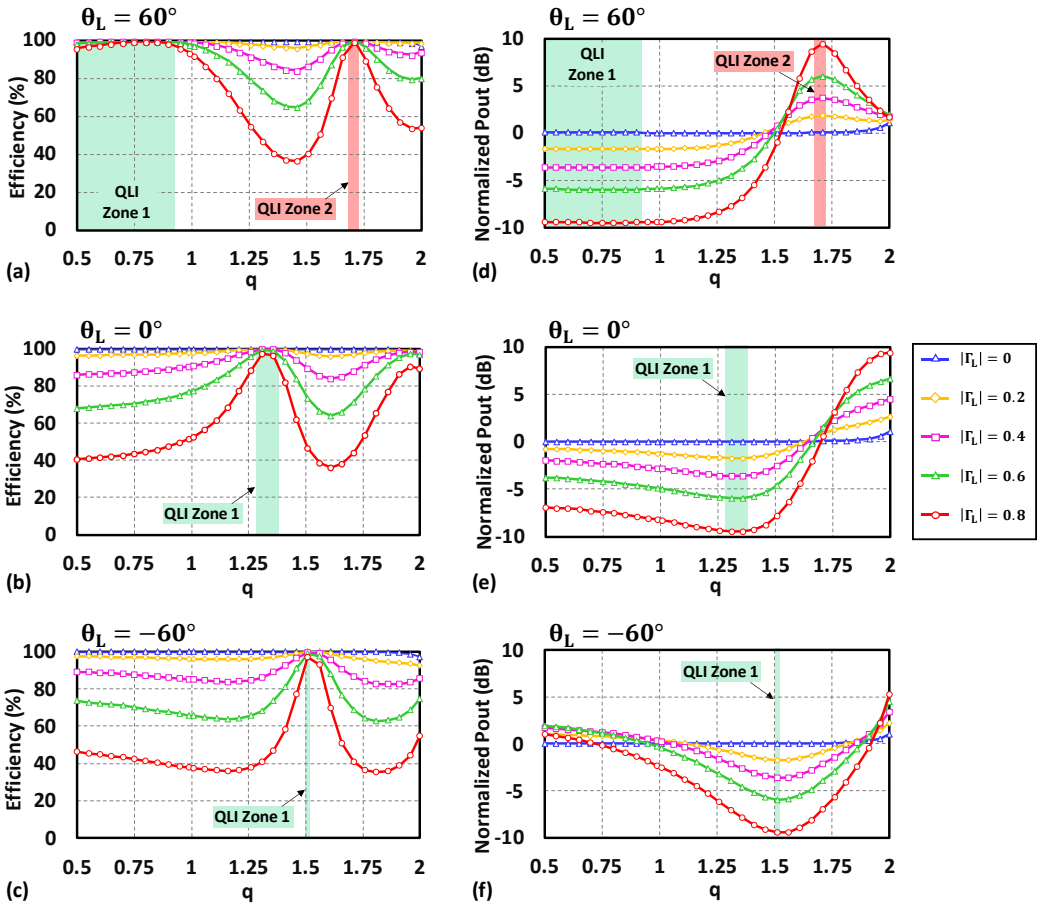

Figure 7. (a), (b), (c): Efficiency and (d), (f), (g): normalized output power versus q sampled at different $|\Gamma_L|$ and for θ_L=60°,0° and -60°. $\alpha = 0$.

The data on **Figure *7*** shows that depending on the value of $\boldsymbol{\theta_L}$ the range of $\boldsymbol{q}$ values where the class-E network is QLI (named the QLI zone) changes. All these QLI zones are suitable to design load modulated PAs since the efficiency remains high and the output power varies with $|\boldsymbol{\Gamma_L}|$. Note that, for positive $\boldsymbol{\theta_L}$ there exists two QLI zones as shown in **Figure *7*** (a) and (d). the QLI zone 1 has an increasing output power as $|\boldsymbol{\Gamma_L}|$ decrease while the QLI zone 2 has a decreasing output power, **Figure *7*** (d). To address any QLI zone for load modulated PAs, the load impedance trajectory presented by the combiner must be such as the output power increases. Hence, the angle on the smith chart of the load impedance trajectory to address the QLI zone 2 should be $\theta_L - 180°$ to obtain increasing output power.

The generalized class-E network, **Figure *1***, allows to take into account a series inductance $\boldsymbol{L_b}$ when designing a class-E network by considering $\boldsymbol{\alpha \geq 0}$ ($\boldsymbol{\alpha = L_b/L_1}$). For a given $\boldsymbol{q}$, changing $\boldsymbol{\alpha}$ will change the $\boldsymbol{\theta_L}$ for QLI operation (named $\boldsymbol{\theta_{L|QLI}}$). This can be observed on the extracted $\boldsymbol{\theta_{L|QLI}}$ from the loadpull simulation for $\boldsymbol{q}$ from 0.5 to 2 and $\boldsymbol{\alpha}$ from 0 to 1 in **Figure *8*** (a). As can be seen in **Figure *8*** (a), $\boldsymbol{\theta_L}$ remains almost constant for $\boldsymbol{q < 1}$, while for $\boldsymbol{q > 1}$ $\boldsymbol{\theta_L}$ is more sensitive to $\boldsymbol{q}$ (i.e., to network parameters values). This suggests that a QLI class-E DPA with $\boldsymbol{q < 1}$ has more potential for wideband operation and is more robust against process variation. Moreover, increasing $\boldsymbol{\alpha}$ increase

$\boldsymbol{\theta_{L|QLI}}$ for a given $\boldsymbol{q}$. As one can observe, the increase of $\boldsymbol{\theta_{L|QLI}}$ with $\boldsymbol{\alpha}$ becomes insignificant for lower $\boldsymbol{q}$ values. This means that for a given low $\boldsymbol{q}$ value, a series inductance $\boldsymbol{L_b}$ can be added without affecting $\boldsymbol{\theta_{L|QLI}}$.

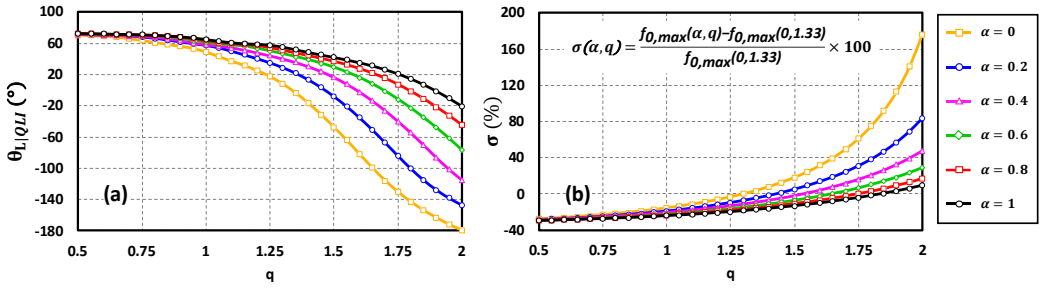

Figure 8. (a) $\theta_{L|QLI}$ versus q for $\alpha = [0:1]$ step 0.2, (b) normalized deviation of $f_{0,max}$ (α, q) with respect to $f_{0,max}$ $(0, q = 1.33)$ for $\alpha = [0:1]$ step 0.2.

An equation of $\boldsymbol{\theta_{L|QLI}(\alpha, q)}$ has been fitted in the range of **Figure** *8* (a) in (5) allowing for a given $\boldsymbol{q}$ and $\boldsymbol{\alpha}$ to predict the angle suitable for QLI operation.

$$\theta_{L|QLI}(\alpha, q) = -34.37q^3 - 17.51q^2 + 38.25q + 20.28\alpha^3 + 11.8\alpha^2 + 3.36\alpha + 93.1q^2\alpha - 69.9q\alpha^2 - 39.6q\alpha + 60.25 \quad (5)$$

Unfortunately, selecting a given $\boldsymbol{q}$ and $\boldsymbol{\alpha}$ value to align the power and efficiency contours in a given direction will affect the maximum design frequency ($\boldsymbol{f_{0,max}}$) of the class-E PA. As mentioned in [7], $\boldsymbol{f_{0,max}}$ is defined as the design frequency at which the capacitance $\boldsymbol{C_1}$ becomes lower than the device output capacitance ($\boldsymbol{C_{dev}}$). Hence, by substituting $\boldsymbol{C_1}$ by $\boldsymbol{C_{dev}}$, $\boldsymbol{f_{0,max}}$ can be expressed as follow:

$$f_{0,max}(\alpha, q) = \frac{K_c(\alpha, q)\, P_{out}}{2\pi\, K_p(\alpha, q)\, V_{dd}^2 C_{dev}} = \frac{P_d}{2\pi\, V_{dd}^2 C_u} \frac{K_c(\alpha, q)}{K_p(\alpha, q)} \quad (6)$$

Where $\mathbf{P_d}$ and $\mathbf{C_u}$ are the power density (in W/mm) and normalized output capacitance (in F/mm) for a given technology, which are almost constant for a given process and under a given $\mathbf{V_{dd}}$. According to (6), for a given process and under a given $\mathbf{V_{dd}}$, increasing the design parameter $\boldsymbol{q}$ allows addressing higher operating frequency, regardless of the target $\boldsymbol{P_{out}}$ as can be seen on **Figure** *8* (b), which shows the normalized deviation $\boldsymbol{\sigma(\alpha, q)}$ of $\boldsymbol{f_{0,max}(\alpha, q)}$ with respect to $\boldsymbol{f_{0,max}(0, q = 1.33)}$. Additionally, reducing the series inductance $\boldsymbol{L_b}$ (i.e., reducing $\boldsymbol{\alpha}$) for a given $\boldsymbol{q}$ tends to increase the maximum operating frequency. Hence, the choice of $\boldsymbol{q}$ and $\boldsymbol{\alpha}$ should be a tradeoff between the desired $\boldsymbol{\theta_{L|QLI}}$ and the targeted operating frequency, $\boldsymbol{f_{0,max}}$. To decorrelate the choice of $\boldsymbol{\theta_{L|QLI}}$ and $\boldsymbol{f_{0,max}}$.

To reduce the constraints related to the choice of $\boldsymbol{\alpha}$ and $\boldsymbol{q}$, a transmission line (TL) with a characteristic impedance $\boldsymbol{R(\alpha, q)}$ and an electrical length $\boldsymbol{\theta_x}$ is added between $\boldsymbol{Z_L = R(\alpha, q)}$ and the class-E network, as shown in **Figure** *9*. Since the loadpull contours are normalized to $\boldsymbol{R(\alpha, q)}$, the transmission line will rotate the loadpull contours by $\boldsymbol{\theta_x}$ according to the following equation:

$$\Gamma_{L,ce} = |\Gamma_L|\, e^{j(\theta_{L|QLI} + 2\theta_x)} \quad (7)$$

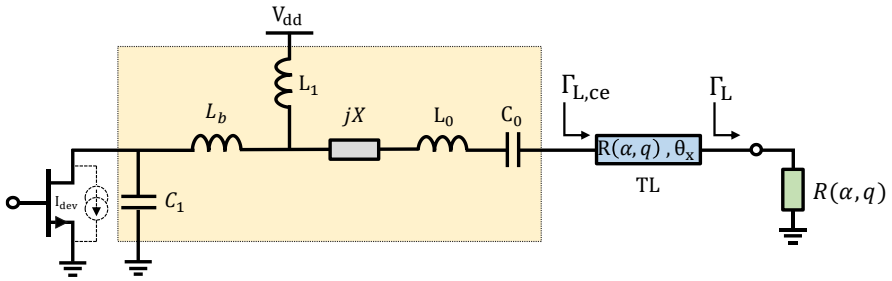

Figure 9. *Class-E PA with output transmission line.*

Thus, with this additional degree of freedom, the power and efficiency contours can be oriented in any direction regardless of the choice of $\boldsymbol{q}$ and $\boldsymbol{\alpha}$. Hence, the designer can match the class-E PA contours orientation to the load modulated impedance trajectories required by any Doherty combiner while selecting the class-E network parameters $\boldsymbol{q}$ and $\boldsymbol{\alpha}$ based on other design criteria such as operating frequency, bandwidth, network components quality factor and size. For illustration, **Figure *10*** shows that for $\boldsymbol{\theta_x = 40°}$ the power and efficiency contours can be rotated from the real impedance axis (for $\boldsymbol{\theta_x = 0°}$, $\boldsymbol{q = 1.33}$ and $\boldsymbol{\alpha = 0}$) as to match the impedance trajectories required by the compact L-C Doherty combiner (shown on **Figure *5*** (a)).

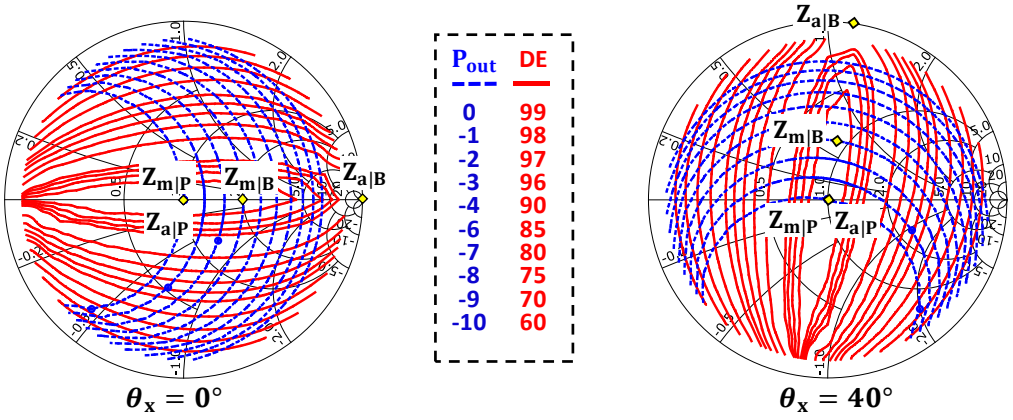

Figure 10. Output power and efficiency contours of ideal class-E PA with $q = 1.33$ and $\alpha = 0$ considering: (a) θ_x=0°, (b) θ_x=40°.

Now the choice of $\boldsymbol{\theta_{L|QLI}}$ and $\boldsymbol{f_{0,max}}$ can be decorrelate using this output TL. However, at low power region when the Auxiliary is off, this TL can transform the off-state impedance of the auxiliary class-E PA leading to a back-off performance degradation. The next subsection investigates the impact of the choice of q and α on the auxiliary off-State impedance.

3.3 Impact of the Choice of $\boldsymbol{q}$ and $\boldsymbol{\alpha}$ on the Auxiliary Off-State Impedance.

In the low power region, the auxiliary PA is off and only the main PA delivers power to the load. When the auxiliary is off, ideally its off-state impedance is infinite ($\boldsymbol{Z_{off} = \infty}$) and assuming that the Output Matching Network (OMN) is lossless no power can be dissipated on the auxiliary path. However, in a practical case with a real transistor, this off-state impedance is not infinite and the power delivered by the main PA can be dissipated in the auxiliary path. In this case, the design of the auxiliary OMN ($OMN_{a|ce}$) is critical to mitigate the losses in the auxiliary path. In fact, the impedance presented at the combiner plane $\boldsymbol{Z_{a|off_{ce}}}$, in **Figure *11*** (a), can be derived using the $OMN_{a|ce}$ ABCD matrix ($[ABCD]_{OMN_{a|ce}}$) as follows:

$$Z_{a|off_{ce}} = \frac{B_a + D_a Z_{off}}{A_a + C_a Z_{off}} \quad (8)$$

Considering a class-E Doherty PA design, for a given $\boldsymbol{P_{out}}$, $\boldsymbol{V_{dd}}$, $\boldsymbol{f_0}$ and $\boldsymbol{Q_L}$ the choice of $\boldsymbol{\alpha}$ and $\boldsymbol{q}$ affects the coefficient of $[ABCD]_{OMN_{a|ce}}$ changing the impedance presented at the coupler's plane $\boldsymbol{Z_{a|off_{ce}}}$. Moreover, the combiner transforms (through OMN_a) $\boldsymbol{Z_{a|off_{ce}}}$ in $\boldsymbol{Z_{a|off}}$ which is the off-state impedance in parallel with the load $\boldsymbol{Z_L}$. The parallel resistance of $\boldsymbol{Z_{a|off}}$, $\boldsymbol{R_{a|off}}$, has to be much larger than $\boldsymbol{Z_L}$ to not affect the back-off performances.

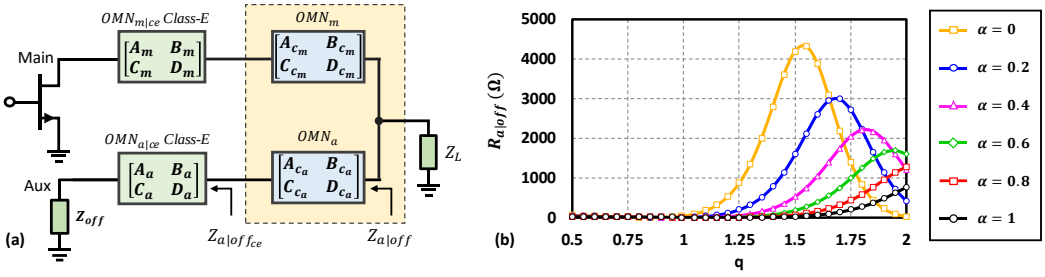

Figure 11. (a) *Block schematic of class-E Doherty PA in the low power region. (b)* $Z_{a|off}$ *versus* α *and* q.

To illustrate that, in the case of a conventional Doherty combiner (OMN_a is just a wire), the off-state impedance of the commercial device **CG2H40015D** is extracted ($\boldsymbol{Z_{off} = 0.29 - j29.5}$). Then, $\boldsymbol{Z_{a|off} = Z_{a|off_{ce}}}$ is computed for $\boldsymbol{P_{out} = 15\,W}$, $\boldsymbol{V_{dd} = 28\,V}$, $\boldsymbol{f_0 = 3.8\,GHz}$ and $\boldsymbol{Q_L = 30}$. After, the parallel resistance ($\boldsymbol{R_{a|off}}$) is calculated and plotted in **Figure *11*** (b) versus $\boldsymbol{q}$ for several $\boldsymbol{\alpha}$. As one can observe, increasing $\boldsymbol{\alpha}$ tends to reduce $\boldsymbol{R_{a|off}}$ for a given $\boldsymbol{q}$. Moreover, there is an optimal choice for $\boldsymbol{q}$ that achieves the highest parallel resistance. The highest parallel resistance is achieved for $\boldsymbol{\alpha = 0}$ and $\boldsymbol{q = 1.53}$ suggesting that this configuration is the best to reduce the performance drop due to the off-state impedance in the low power region. Moreover, for low $\boldsymbol{q}$ values, $\boldsymbol{R_{a|off}}$ drops drastically increasing the power injected to the auxiliary path and increases the losses. Thus, $\boldsymbol{\alpha}$ and $\boldsymbol{q}$ has to be selected carefully in respect with the desired combiner to reduce the losses in the auxiliary path.

The upcoming section illustrates the proposed class-E Doherty methodology using the **CG2H40015D** devices.

4. Application of the Proposed Design Methodology

To validate the extended design methodology, two QLI class-E Doherty PA designs with a L-C combiner are proposed using the **CG2H80015D** commercial GaN HEMT transistor with two configurations for both designs, **Figure *12***. In the first design, as in our previous paper [11], the class-E network ($\boldsymbol{\alpha = 0}$)with output TL is used. In the second design, we utilize the generalized class-E network taking advantage of the contours rotation with $\boldsymbol{\alpha}$ presented in section 3.2. The designs target 6-dB OBO and 40 W (46 dBm) of peak output power under 28 V supply voltage at 3.8 GHz. Since the OBO targeted is 6-dB, each PA delivers 20 W at peak output power. One configuration is done for $\boldsymbol{q = 0.9}$ where $\boldsymbol{\theta_{L|QLI}}$ is directly aligned with the load impedance trajectory of L-C combiner (i.e., $\theta_L = 60°$). The second configuration is done for $\boldsymbol{q = 1.33}$ and $\boldsymbol{\theta_{L|QLI}}$ need to be ajusted. The main device is biased at -2.9 V and the auxiliary at -5.5 V. Note that in practical design the input signal drive is sinusoidal and the device has a non-zero knee voltage and nonlinear output capacitance. Moreover, for the targeted design, the parallel capacitance of the network, C_1, remains lower than the device's output capacitance leading to a suboptimum operation of class-E. Consequently, a tuning factor $\boldsymbol{K_R}$ is introduced to account for

these non-idealities. Therefore, $\boldsymbol{R(\alpha, q)}$ is now expressed as in (9), while other equations remain unchanged.

$$R(\alpha, q) = K_R \frac{K_P(\alpha, q)\, V_{dd}^2}{P_{out}} \tag{9}$$

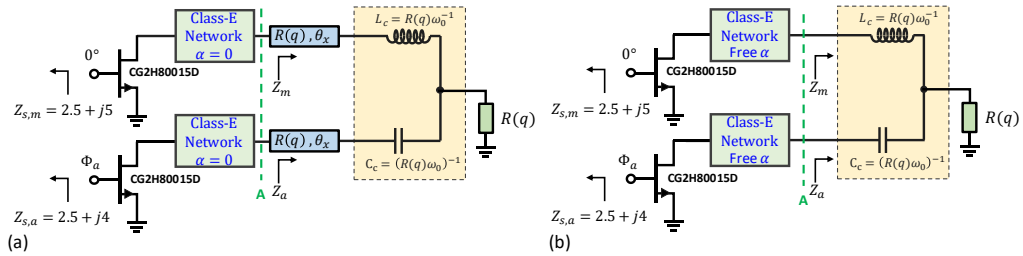

Figure 12. (a) Proposed class-E Doherty PA using L-C combiner (with $\alpha = 0$) (b) Proposed generalized class-E Doherty PA using L-C combiner.

First design uses the network of our previous paper (**Figure *12*** (a)) with $\boldsymbol{\alpha = 0}$ (i.e., $\boldsymbol{L_b = 0}$). The output power and efficiency contours are plotted at plane A considering $\boldsymbol{K_R = 0.375}$ for $\boldsymbol{q = 0.9}$ and $\boldsymbol{K_R = 0.395}$ for $\boldsymbol{q = 1.33}$ and follow the same trend as the theoretical ones. Note that the input phase has been slightly adjusted to achieve proper load modulation ($\boldsymbol{\Phi_a = -105°}$ for $\boldsymbol{q = 0.9}$ and $\boldsymbol{\Phi_a = -100°}$ for $\boldsymbol{q = 1.33}$). For $\boldsymbol{q = 1.33}$, $\boldsymbol{\theta_x}$ is tuned to 45° to align the load impedance trajectories with the contours while for $\boldsymbol{q = 0.9}$ the contours are aligned with the load impedance trajectory leading to $\boldsymbol{\theta_x = 0}$. The proposed QLI class-E DPA design is validated using large signal harmonic balance simulation using the **CG2H80015D** model provided by MACOM and considering a lossy output network with a quality factor of 60 for inductors and 90 for capacitors. As shown in **Figure *13***, both designs achieve proper load modulation since the trajectories of $\boldsymbol{Z_m}$ and $\boldsymbol{Z_a}$ cross the desired $\boldsymbol{P_{out}}$ levels inside the high efficiency contours region.

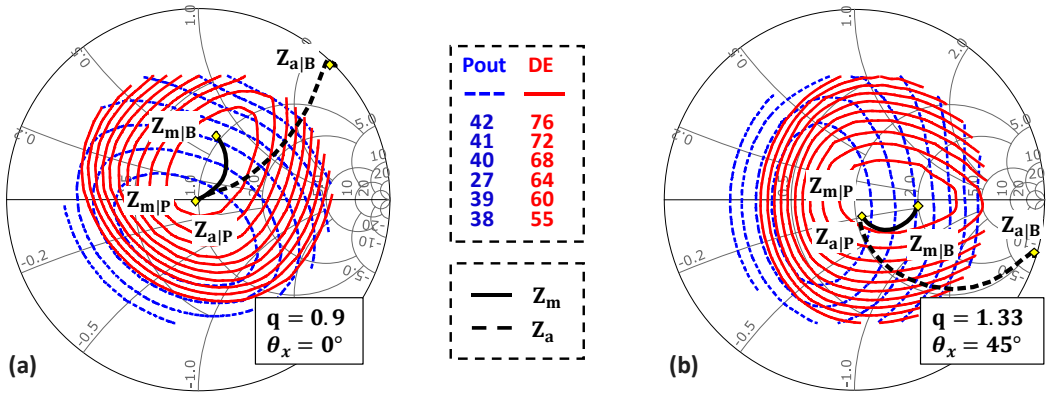

Figure 13. Power and efficiency load-pull contours, Z_m and Z_a at plane A for: (a) $q = 0.9$ and $\theta_x = 0°$, (b) $q = 1.33$ and $\theta_x = 45°$.

As shown on **Figure *14***, both DPAs achieve a saturated output power of 46 dBm with more than 70% drain efficiency (DE) over the 6-dB OBO and a large signal gain around 13 dB.

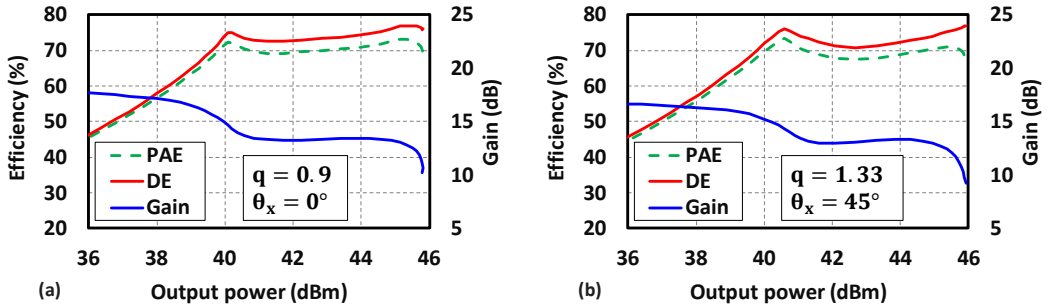

Figure 14. Simulated performance of the QLI class-E Doherty PAs with L-C combiner for: (a) q = 0.9 and $\theta_x = 0°$, (b) q = 1.33 and $\theta_x = 45°$.

In the second design (**Figure *12*** (b)), the generalized class-E network is used. For this network, the output TL in **Figure *9*** is not necessary to rotate the loadpull contours since the inductance $\boldsymbol{L_b}$ can do it. A bond wire is used to connect the commercial die to output matching network. In the following, we assume that the inductance $\boldsymbol{L_b}$ added by the bond wire can be controlled in the process.

The output power and efficiency contours are plotted at plane A in **Figure *15***, considering $\boldsymbol{K_R = 0.375}$ for $\boldsymbol{q = 0.9}$ and $\boldsymbol{K_R = 0.395}$ for $\boldsymbol{q = 1.33}$. Note that the input phase has been slightly adjusted to achieve proper load modulation ($\boldsymbol{\Phi_a = -105°}$ for $\boldsymbol{q = 0.9}$ and $\boldsymbol{\Phi_a = -105°}$ for $q = \boldsymbol{1.33}$). For $\boldsymbol{q = 0.9}$, the bond wire can be added without affecting $\boldsymbol{\theta_L}$ since $\boldsymbol{\alpha}$ has almost no effect on $\boldsymbol{\theta_L}$ as presented in **Figure *8*** (a). Thus $\boldsymbol{\alpha}$ is selected to 0.25 to present an achievable bond wire inductance of $\boldsymbol{L_b = 0.7\ nH}$. For $\boldsymbol{q = 1.33}$, $\boldsymbol{\alpha}$ affects the QLI operation angle. Hence, using (6) $\boldsymbol{\alpha}$ is selected to 0.5 ($\boldsymbol{L_b = 0.6\ nH}$) in order to align the contours with the load modulation of the L-C combiner. The proposed QLI class-E DPA design is validated as previously done in simulation. As shown in **Figure *15***, both designs achieve proper load modulation since the trajectories of $\boldsymbol{Z_m}$ and $\boldsymbol{Z_a}$ cross the desired $\boldsymbol{P_{out}}$ levels inside the high efficiency contours region.

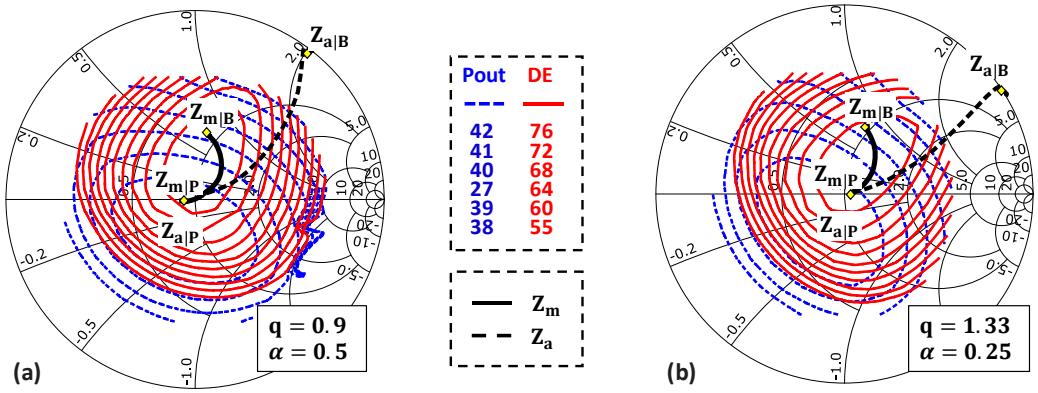

Figure 15. Power and efficiency load-pull contours, Z_m and Z_a at plane A for: (a) $q = 1.33$ and $\alpha = 0.5$, (b) $q = 0.9$ and $\alpha = 0.25$.

As shown on **Figure *16***, both DPAs achieve a saturated output power of 46 dBm with more than 70% drain efficiency (DE) over the 6-dB OBO and a large signal gain around 13 dB.

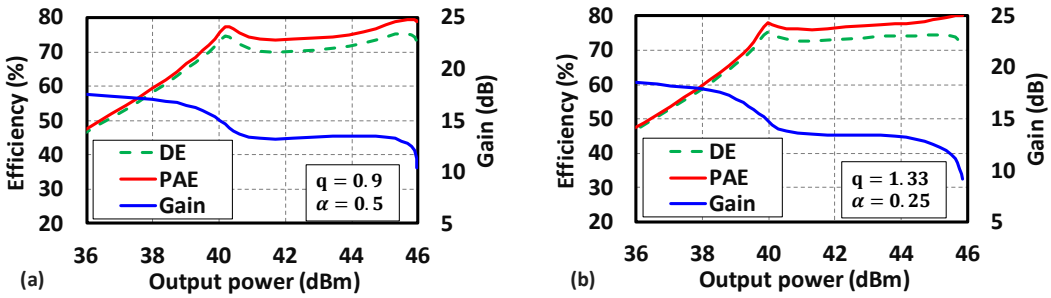

Figure 16. Simulated performance of the QLI class-E Doherty PAs with L-C combiner for: (a) q = 0.9 and $\alpha = 0.5$, (b) q = 1.33 and $\alpha = 0.25$.

Hence, the proposed extended methodology for QLI class-E design is validated. The simulations results validated the proposed methodology showing that the uses of output transmission line and a wisely chosen α can allow to decorrelate the choice of q and the combiner choice in a practical case.

4. Conclusion

In conclusion, this study extends the QLI Class-E Doherty PA design for complex load impedance trajectories and generalized class-E network. It allows designing high efficiency Doherty PA using combiners that present a complex-to-real impedance trajectory. Adjusting the class-E network resonance factor $\boldsymbol{q}$ and the series inductance $\boldsymbol{L_b}$ enables QLI operation with various types of Doherty combiner. A fitted equation for the QLI angle is provided allowing to predict the angle of QLI operation for any $\mathbf{q}$ and $\boldsymbol{\alpha}$ in the given range. A novel approach using a transmission line at the output of class-E network mitigates the maximum operating frequency limitation caused by the resonance factor and series inductance choice and reduces the constraint on the choice of $\boldsymbol{q}$ and $\boldsymbol{\alpha}$. Then, the impact of $\boldsymbol{q}$ and $\boldsymbol{\alpha}$ on the auxiliary off-state impedance has been investigated for a conventional Doherty combiner. Finally, the methodology is validated on two different 40 W Doherty PA designs. One is using the proposed output transmission line approach considering no series inductance (i.e., $\boldsymbol{\alpha = 0}$) and the second is taking advantage of the series inductance $\boldsymbol{L_b}$. All the designed class-E Doherty PAs achieve over 70% efficiency across a 6-dB output power back-off at 3.8 GHz in simulation.

The proposed analysis is done at a single frequency. Nevertheless, to meet the requirements of 5G applications, the PAs has to operate over a large bandwidth. Hence, the impact of $\boldsymbol{q, \alpha}$ and the combiner for broadband operation must be investigated.

Author Contributions: Conceptualization, Mehdi Otmani and Ayssar Serhan; Methodology, Mehdi Otmani and Ayssar Serhan; Supervision, Ayssar Serhan, Jean-Daniel Arnould and Estelle Lauga-Larroze; Visualization, Alexandre Giry; Writing – original draft, Mehdi Otmani; Writing – review & editing, Ayssar Serhan, Jean-Daniel Arnould, Estelle Lauga-Larroze, Pascal Reynier and Alexandre Giry.

Funding: This work was supported by the ANR under the France 2030 program, grant NF-PERSEUS: ANR-22-PEFT-0004.

Conflicts of Interest: The authors declare no conflicts of interest.

References

1. A. Giry, A. Serhan, D. Parat, and P. Reynier, "Linear Power Amplifiers for Sub-6GHz Mobile Applications : Progress and Trends," in *2020 18th IEEE International New Circuits and Systems Conference (NEWCAS)*, Montréal, QC, Canada: IEEE, Jun. 2020, pp. 226–229. doi: 10.1109/NEWCAS49341.2020.9159835.
2. W. H. Doherty, "A New High Efficiency Power Amplifier for Modulated Waves," *Proc. IRE*, vol. 24, no. 9, pp. 1163–1182, Sep. 1936, doi: 10.1109/JRPROC.1936.228468.
3. M. Ozen, M. van der Heijden, M. Acar, R. Jos, and C. Fager, "A Generalized Combiner Synthesis Technique for Class-E Outphasing Transmitters," *IEEE Trans. Circuits Syst. Regul. Pap.*, vol. 64, no. 5, pp. 1126–1139, May 2017, doi: 10.1109/TCSI.2016.2636155.
4. N. Srirattana, A. Raghavan, D. Heo, P. E. Allen, and J. Laskar, "Analysis and design of a high-efficiency multistage Doherty power amplifier for wireless communications," *IEEE Trans. Microw. Theory Tech.*, vol. 53, no. 3, pp. 852–860, Mar. 2005, doi: 10.1109/TMTT.2004.842505.
5. J. H. Qureshi, W. Sneijers, R. Keenan, L. C. N. deVreede, and F. van Rijs, "A 700-W peak ultra-wideband broadcast Doherty amplifier," in *2014 IEEE MTT-S International Microwave Symposium (IMS2014)*, Tampa, FL, USA: IEEE, Jun. 2014, pp. 1–4. doi: 10.1109/MWSYM.2014.6848495.
6. A. R. Qureshi, M. Acar, S. C. Pires, and L. C. N. de Vreede, "High Efficiency and Wide Bandwidth Quasi-Load Insensitive Class-E Operation Utilizing Package Integration," *IEEE Trans. Microw. Theory Tech.*, vol. 66, no. 12, pp. 5310–5321, Dec. 2018, doi: 10.1109/TMTT.2018.2868876.
7. X. A. Nghiem and J. Gajadharsing, "Continuous Quasi-Load Insensitive Class-E Mode for Wideband Doherty Power Amplifiers," in *2023 IEEE/MTT-S International Microwave Symposium - IMS 2023*, San Diego, CA, USA: IEEE, Jun. 2023, pp. 450–453. doi: 10.1109/IMS37964.2023.10188219.
8. J. Bachi *et al.*, "A Novel Approach for Doherty PA Design Using a Compact L-C Combiner," *IEEE Trans. Circuits Syst. II Express Briefs*, vol. 69, no. 10, pp. 4023–4027, Oct. 2022, doi: 10.1109/TCSII.2022.3185174.
9. C. Rong, X. Liu, Y. Xu, and M. Xia, "Analysis and Design of Class E Power Amplifier with Finite DC-Feed Inductance and Series Inductance Network," *ACES J. Pap.*, vol. 32, no. 5, 2017.
10. M. Acar, A. J. Annema, and B. Nauta, "Analytical Design Equations for Class-E Power Amplifiers," *IEEE Trans. Circuits Syst. Regul. Pap.*, vol. 54, no. 12, pp. 2706–2717, Dec. 2007, doi: 10.1109/TCSI.2007.910544.
11. M. Otmani, A. Serhan, J.-D. Arnould, E. Lauga-Larroze, and A. Giry, "Extension of Quasi-Load Insensitive Class-E Doherty Operation with Complex Load Trajectories," in *2024 19th Conference on Ph.D Research in Microelectronics and Electronics (PRIME)*, Larnaca, Cyprus: IEEE, Jun. 2024, pp. 1–4. doi: 10.1109/PRIME61930.2024.10559702.
12. K. Takenaka, T. Sato, H. Matsumoto, M. Kawashima, and N. Nakajima, "New compact Doherty power amplifier design for handset applications," in *2017 IEEE Topical Conference on RF/Microwave Power Amplifiers for Radio and Wireless Applications (PAWR)*, Phoenix, AZ, USA: IEEE, Jan. 2017, pp. 81–83. doi: 10.1109/PAWR.2017.7875579.